Vol. 80, No. 2

Nucleocytoplasmic Shuttling of Bovine Herpesvirus 1 UL47 Protein in Infected Cells

Janneke Verhagen, Ian Hutchinson, and Gillian Elliott*

Virus Assembly Group, Marie Curie Research Institute, Oxted, Surrey, United Kingdom

Previous studies with transfected cells have shown that the herpes simplex virus type 1 (HSV-1) and bovine herpesvirus 1 (BHV-1) UL47 proteins shuttle between the nucleus and the cytoplasm. HSV-1 UL47 has also been shown to bind RNA. Here we examine the BHV-1 UL47 protein in infected cells using a green fluorescent protein-UL47-expressing virus. We show that UL47 is detected in the nucleus early in infection. We use fluorescence loss in photobleaching to show that nuclear UL47 undergoes rapid nucleocytoplasmic shuttling. Furthermore, we demonstrate that actinomycin D inhibits the reaccumulation of UL47 in the nuclei of infected cells. These results suggest that UL47 exhibits behavior similar to that of previously characterized RNA-transporting proteins.

The alphaherpesvirus UL47 gene encodes a protein that is assembled into the tegument of the virion (1, 7, 10, 23). While the role of UL47 has not yet been defined, its deletion from herpes simplex virus type 1 (HSV-1), pseudorabies virus, or Marek's disease virus results in viruses that produce small plaques and replicate more slowly than wild-type (Wt) viruses (4, 7, 24, 25). We have previously studied the HSV-1 UL47-encoded protein VP13/14 expressed in infected cells and by transient transfection. In both cases, VP13/14 was targeted to the nucleus, and we have identified an arginine-rich nuclear localization signal in its N terminus (2, 3). Furthermore, we have shown that VP13/14 has the ability to shuttle between the nucleus and the cytoplasm when expressed alone (3).

The bovine herpesvirus 1 (BHV-1) homologue of VP13/14, the UL47-encoded protein VP8, is by far the major structural protein of the BHV-1 virus particle (1), and as yet there has been no report of a UL47 knockout virus for BHV-1. Immunofluorescence studies of infected cells have shown VP8 in the nucleus (22), and a recent study demonstrated that as for VP13/14, VP8 appears to shuttle between the nucleus and the cytoplasm when expressed in isolation (26). Here we have examined the trafficking of the BHV-1 UL47 protein in infected cells by constructing a recombinant virus expressing green fluorescent protein (GFP)-tagged UL47. Infectious BHV-1 genomic DNA (strain P8-2) was cotransfected into COS-1 cells with plasmid pJV46, which consists of the GFP open reading frame flanked by 1 kb of the UL47 upstream sequence and the entire UL47 open reading frame. Green fluorescent plaques were purified three times on MDBK cells, resulting in the recombinant virus jv46v (Fig. 1A). The growth characteristics of jv46v were established by conducting a time course of infection with MDBK cells. Total cell lysates were analyzed by sodium dodecyl sulfate-polyacrylamide gel electrophoresis (SDS-PAGE) and Western blotting with a polyclonal anti-BHV-1 UL47 antibody, indicating that the UL47-

reactive species in jv46v-infected cells was around 30 kDa larger than Wt UL47 (Fig. 1B). This species also reacted with a monoclonal GFP antibody (Clontech), confirming that it represented a novel GFP-UL47 fusion protein (Fig. 1B). Importantly, the rates of expression of UL47 in the two viruses were similar, as were the expression kinetics of the bTIF protein encoded by UL48 (Fig. 1B). One-step growth curves for intracellular and extracellular virus also indicated that the introduction of GFP at the N terminus of UL47 had no effect on virus replication (Fig. 1C). Importantly, the recombinant virus also exhibited the same plaque size and the same replication rate under low-multiplicity conditions as the Wt virus (data not shown).

We next addressed the assembly of GFP-UL47 into extracellular virions that had been purified from 5×10^8 infected MDBK cells. Wt and jv46v virions were isolated by centrifugation through a 5 to 15% Ficoll gradient and were analyzed by SDS-PAGE followed by Coomassie blue staining or Western blotting. The high level of UL47 is obvious from the protein profile of Wt BHV-1 virions (Fig. 2A). Furthermore, the profile of jv46v BHV-1 virions shows that the 105-kDa VP8 protein has been replaced by a larger species of around 135 kDa (Fig. 2A). Western blotting with anti-UL47 and anti-GFP antibodies revealed that this novel component was GFP-UL47 and that it was packaged into the virus particle in amounts equivalent to those of native UL47 (Fig. 2B). To determine if we could establish the fate of virion UL47 at virus entry, MDBK cells were infected with jv46v in the presence of cycloheximide (CHX) (100 µg/ml) and examined live 1 h later. GFP-UL47 was clearly localized in the nucleus of these cells, demonstrating that incoming UL47 was imported into the infected cell nucleus (Fig. 2C). Newly synthesized GFP-UL47 was also detected in the nucleus of infected cells as early as 4 h after infection of MDBK cells in the absence of CHX and increased in intensity until 6 h, when cytoplasmic GFP-UL47 also began to accumulate (Fig. 2D). Over the next 8 h, GFP-UL47 became increasingly cytoplasmic with little detectable nuclear fluorescence (Fig. 2D). The localization of UL47 as determined by the GFP-UL47-expressing virus was similar to that described previously in immunofluorescence studies (22).

* Corresponding author. Mailing address: Virus Assembly Group, Marie Curie Research Institute, Oxted, Surrey RH8 OTL, United Kingdom. Phone: 44 1883 722306. Fax: 44 1883 714375. E-mail: g .elliott@mcri.ac.uk.
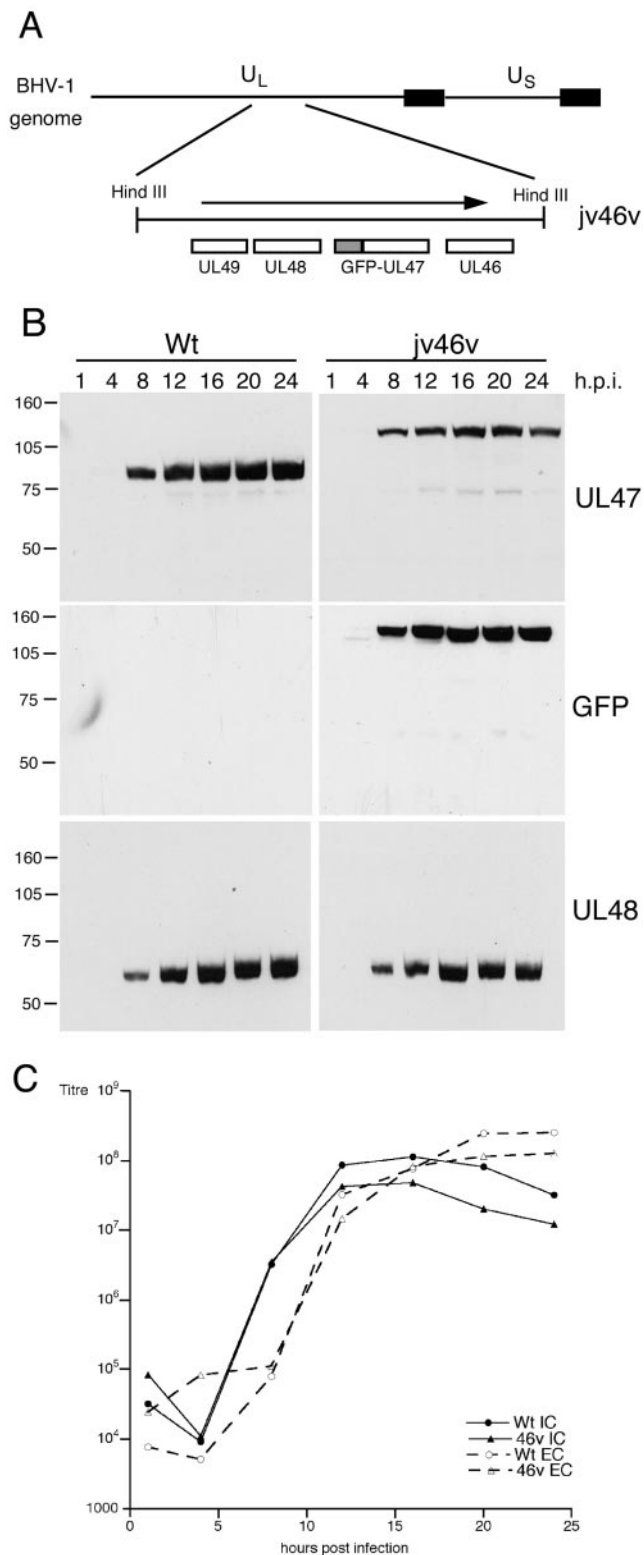
FIG. 1. Insertion of GFP at the N terminus of UL47 has no effect on BHV-1 replication. (A) To construct a plasmid expressing GFP-UL47, the UL47 open reading frame was first transferred as a BamHI/XhoI fragment from plasmid pcVP8, in which the BamHI site is located seven bases upstream of the initiation codon (kindly provided by Vikram Misra, University of Saskatchewan) into pcDNAI/Amp. VP8 was then inserted into pEGFPC1 (Clontech) as a BamHI/XbaI fragment to create pJV2. Finally, 1 kb upstream of the VP8 gene was amplified by PCR from the BHV-1 genome (strain P8-2) as an AseI/AgeI fragment and inserted into AseI/AgeI-digested pJV2, resulting in
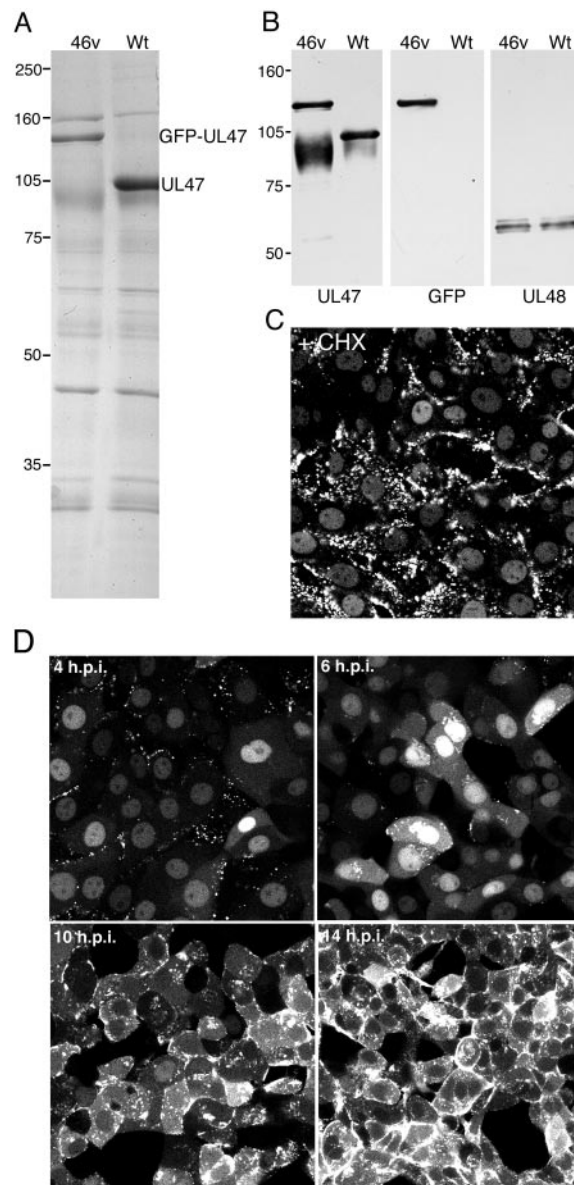

FIG. 2. Characterization of BHV-1 expressing GFP-UL47. (A) Equivalent amounts of extracellular virions purified from Wt- and jv46v-infected MDBK cells were analyzed by SDS-PAGE followed by Coomassie blue staining. (B) The same virions were analyzed by Western blotting with antibodies against UL47, GFP, and UL48. (C) MDBK cells grown in a coverslip chamber were infected with jv46v at a multiplicity of 10 in the presence of 100 μg/ml cycloheximide. One hour later, the cells were imaged on a Zeiss LSM410 confocal microscope. (D) MDBK cells grown in a coverslip chamber were infected with jv46v at a multiplicity of 2. At various times after infection, representative images were collected using a Zeiss LSM410 confocal microscope.

plasmid pJV46 comprising GFP flanked by VP8 upstream sequences at the 5′ end and the VP8 gene at the 3′ end. Cotransfections were then carried out between pJV46 and infectious BHV-1 DNA, and resulting green fluorescent plaques were purified to generate recombinant virus jv46v. (B) MDBK cells infected with either wild-type BHV-1 (Wt) or the GFP-UL47-expressing virus (jv46v) at a multiplicity of 10 were harvested every 4 h up to 24 h after infection. Equal amounts of total cell extracts were analyzed by Western blotting with antibodies against UL47, GFP (Clontech), and UL48. (C) MDBK cells were infected with Wt or jv46v viruses at a multiplicity of 10 and were harvested every 4 h for both intracellular virus (IC) and extracellular virus (EC). Each sample was titrated on MDBK cells.
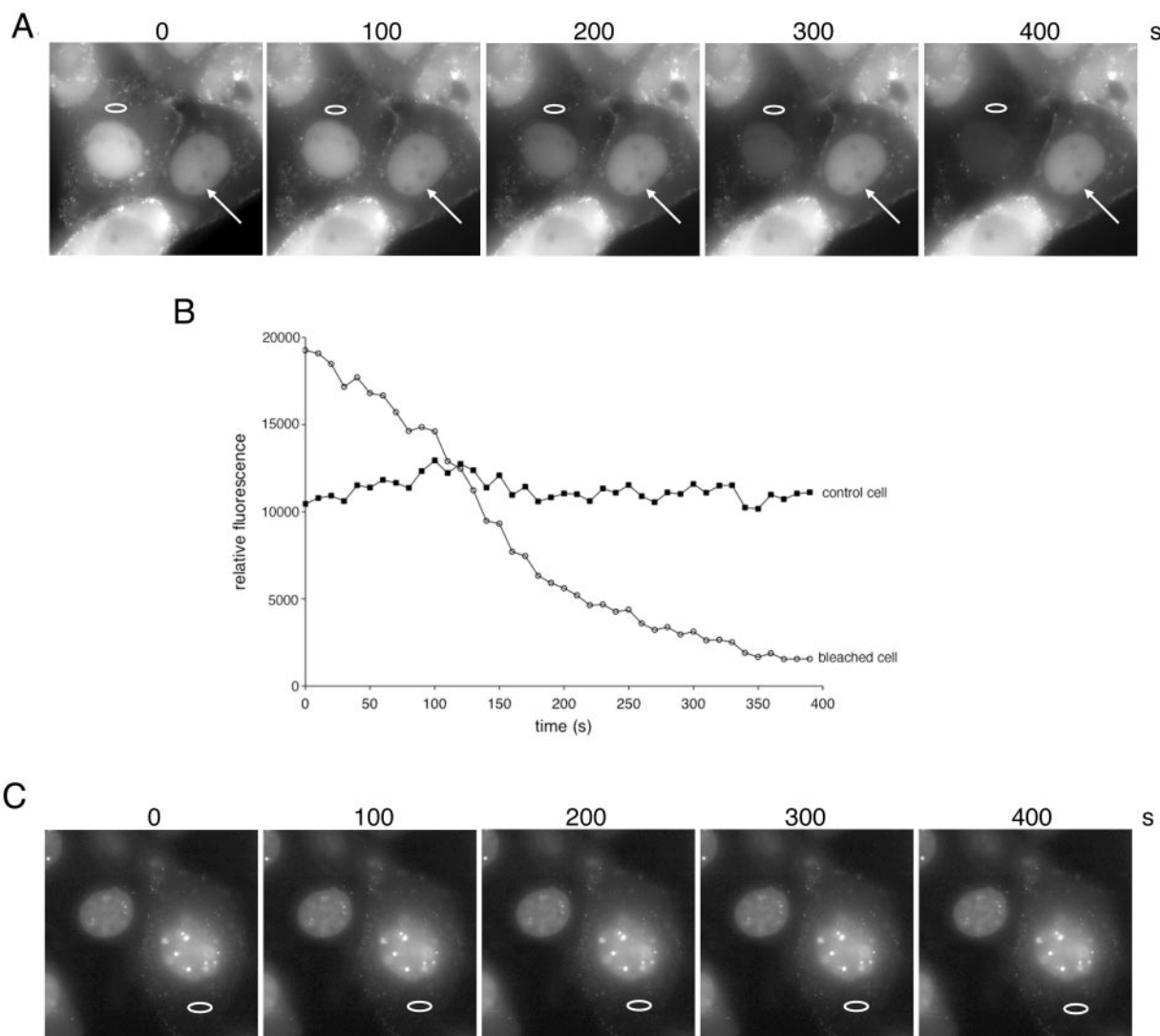
FIG. 3. UL47 shuttles between the nucleus and the cytoplasm in infected cells. (A) MDBK cells grown in a coverslip chamber were infected with jv46v at a multiplicity of 10. At 4 h, the cells were examined using a Deltavision RT imaging system and individual cells chosen for FLIP analysis. The laser module was then used to carry out sequential photobleaching events of the area denoted by the white oval. This area was exposed to the laser for 1 s every 10 s over a period of 7 min. An image of the field was acquired after each bleaching event to determine the loss of fluorescence in the nucleus of the cell. Arrows denote the control cell. (B) The relative fluorescences in the nuclei of the bleached and the unbleached cells in A were quantitated using NIH-image software and plotted against time. (C) MDBK cells infected with HSV-1 expressing GFP-NLS-VP22 in place of Wt VP22 were subjected to FLIP analysis as described for A.

Furthermore, our own comparative immunofluorescence studies between Wt- and jv46v-infected cells using the anti-UL47 antibody confirmed that the addition of GFP to the N terminus of UL47 had no effect on the localization of UL47 (data not shown).

To address the possibility that UL47 may shuttle during virus infection, we employed fluorescence loss in photobleaching (FLIP) technology (6, 8, 17, 21). Four hours after infection, a small area of cytoplasm in jv46-infected MDBK cells was photobleached for 1 s at intervals of 10 s using the laser module on a Deltavision imaging system. In the example shown, which is one of 10 analyses carried out, images of the cell were acquired after each bleach event, resulting in a time-lapse animation that shows a rapid loss of nuclear fluorescence in the bleached

cell compared to the control cell in the same image (Fig. 3A and B). Furthermore, quantification of nuclear GFP-UL47 fluorescence showed that it was reduced to almost background in 7 min (Fig. 3B), suggesting that UL47 export from the nucleus was an extremely rapid event. To confirm that this photobleaching effect was truly indicative of UL47 shuttling, we used a control virus expressing a GFP-tagged protein that is also predominantly nuclear and subjected it to FLIP analysis as described above. For this purpose, we used recombinant HSV-1 that expresses GFP-UL49 (VP22), as described previously (5), but which also has the simian virus 40 nuclear localization signal (NLS) inserted at the N terminus of VP22 (GFP-NLS-VP22). As shown in Fig. 3C (0 s), this results in a GFP-VP22 fusion protein that is predominantly nuclear 4 h
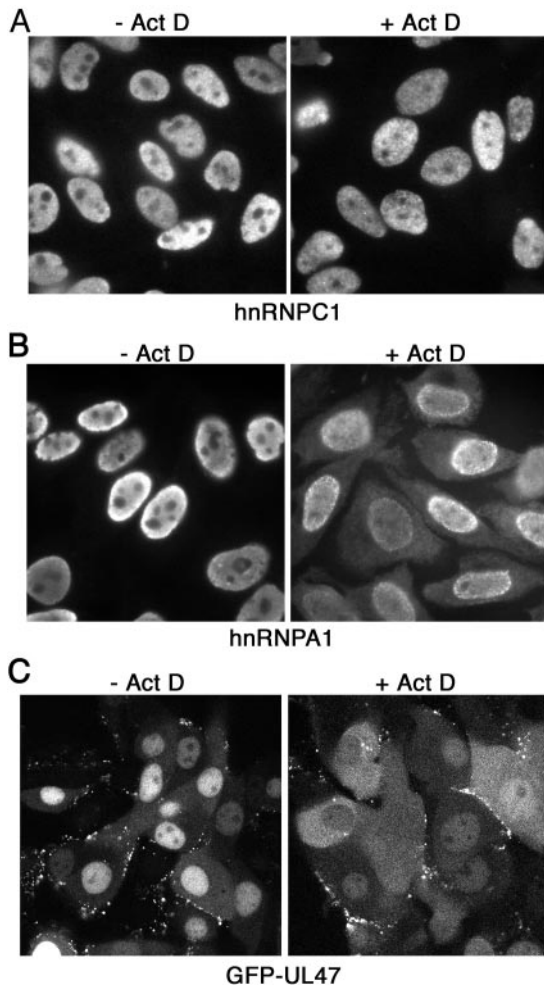
FIG. 4. Actinomycin D treatment inhibits the accumulation of UL47 in the nuclei of infected cells. (A and B) Hep2 cells grown on coverslips were exposed to either 20 μg/ml CHX alone (−Act D) or 20 μg/ml CHX and 5 μg/ml Act D (+Act D) for 3 h prior to fixation with 100% methanol. Immunofluorescence was then carried out with antibodies against either hnRNPC1 (A) or hnRNPA1 (B). (C) MDBK cells grown in a coverslip chamber were infected with jv46v at a multiplicity of 2. Four hours later, the cells were exposed to either 20 μg/ml CHX alone (−Act D) or 20 μg/ml CHX and 5 μg/ml Act D (+Act D). After 1 h, representative images of live cells were acquired using a Zeiss LSM 410 confocal microscope.

after infection, rather than the cytoplasmic localization previously observed for Wt GFP-VP22 (5). Importantly, photobleaching of the cytoplasm of a cell containing nuclear GFP-NLS-VP22 conducted in the same way as for GFP-UL47 had no effect on the level of fluorescence present in the nucleus, thus confirming that the effect we observe with GFP-UL47 is specifically due to its shuttling between the nucleus and cytoplasm. (Fig. 3C).

To further investigate UL47 shuttling, we used the drug actinomycin D (Act D), which affects the shuttling dynamics of many nucleocytoplasmic trafficking proteins and causes the accumulation of such proteins in the cytoplasm rather than the nucleus (12–15). We first tested the experimental conditions for this assay using two endogenous cellular proteins, namely, the known shuttling protein hnRNPA1 and hnRNPC1, a nu-

clear protein that does not shuttle (14–16). Hep2 cells grown on coverslips were treated with CHX alone or CHX and 5 μg/ml Act D, fixed 3 h later in methanol, and processed for immunofluorescence with antibodies against hnRNPA1 and hnRNPC1. As expected, the addition of Act D had no effect on the nuclear localization of hnRNPC1 (Fig. 4A). By contrast, Act D altered the steady-state localization of hnRNPA1 from entirely nuclear to nuclear and cytoplasmic distributions (Fig. 4B), confirming the efficacy of Act D. MDBK cells infected 4 h previously with jv46v were treated in the same way and examined after 1 h. As for hnRNPA1, there was a clear shift of UL47 into the cytoplasm of cells treated with Act D, suggesting that UL47 shuttling was impaired in the presence of Act D (Fig. 4C).

In this study we have provided the first evidence of shuttling by any alphaherpesvirus UL47 gene product during virus infection. This confirms the relevance of previous studies carried out on the nucleocytoplasmic shuttling of UL47-encoded proteins (3, 26). Although the exact role of UL47 shuttling has yet to be determined, it has been reported previously that HSV-1 UL47 binds RNA (19). Here we demonstrate that Act D, a drug that inhibits RNA transcription by RNA polymerase II and is known to inhibit the nuclear reaccumulation of exported RNA binding proteins (15, 16), also alters the localization of UL47. This suggests that UL47 shuttling may be linked in some way to RNA biogenesis. The essential HSV-1 immediate-early protein ICP27 is an RNA binding protein that has already been proposed, among other things, to be involved in the nuclear export of viral RNAs (11, 13, 18, 20). Nonetheless, viruses expressing ICP27 mutated in its RNA binding domain or its nuclear export signal can still replicate, suggesting that this function of ICP27 is not absolutely crucial to the virus (9). It is thus tempting to speculate that UL47 may also function in the export of at least some viral RNAs and that this function may in part compensate for the absence of ICP27-directed RNA export. Furthermore, because UL47 is delivered to the nucleus immediately upon infection, it would be available to function in the transport of the immediate-early viral transcripts. The shift of BHV-1 UL47 steady-state localization from the nucleus to the cytoplasm at later times in infection may simply reflect the high levels of viral RNAs that are being synthesized at this time. However, it may also be indicative of the active recruitment and retention of UL47 in cytoplasmic sites of virus assembly.

REFERENCES

1. **Carpenter, D. E., and V. Misra.** 1991. The most abundant protein in bovine herpes 1 virions is a homologue of herpes simplex virus type 1 UL47. J Gen. Virol. **72:**3077–3084.
2. **Donnelly, M., and G. Elliott.** 2001. Fluorescent tagging of herpes simplex virus tegument protein VP13/14 in virus infection. J. Virol. **75:**2575–2583.
3. **Donnelly, M., and G. Elliott.** 2001. Nuclear localization and shuttling of herpes simplex virus tegument protein VP13/14. J. Virol. **75:**2566–2574.
4. **Dorange, F., B. K. Tischer, J. F. Vautherot, and N. Osterrieder.** 2002. Characterization of Marek's disease virus serotype 1 (MDV-1) deletion mutants that lack UL46 to UL49 genes: MDV-1 UL49, encoding VP22, is indispensable for virus growth. J. Virol. **76:**1959–1970.

5. **Elliott, G., and P. O'Hare.** 1999. Live-cell analysis of a green fluorescent protein-tagged herpes simplex virus infection. J. Virol. **73:**4110–4119.

6. **Griffis, E. R., N. Altan, J. Lippincott-Schwartz, and M. A. Powers.** 2002. Nup98 is a mobile nucleoporin with transcription-dependent dynamics. Mol. Biol. Cell. **13:**1282–1297.

7. **Kopp, M., B. G. Klupp, H. Granzow, W. Fuchs, and T. C. Mettenleiter.** 2002. Identification and characterization of the pseudorabies virus tegument proteins UL46 and UL47: role for UL47 in virion morphogenesis in the cytoplasm. J. Virol. **76:**8820–8833.

8. **Koster, M., T. Frahm, and H. Hauser.** 2005. Nucleocytoplasmic shuttling revealed by FRAP and FLIP technologies. Curr. Opin. Biotechnol. **16:**28–34.

9. **Lengyel, J., C. Guy, V. Leong, S. Borge, and S. A. Rice.** 2002. Mapping of functional regions in the amino-terminal portion of the herpes simplex virus ICP27 regulatory protein: importance of the leucine-rich nuclear export signal and RGG Box RNA-binding domain. J. Virol. **76:**11866–11879.

10. **McLean, G., F. Rixon, N. Langeland, L. Haarr, and H. Marsden.** 1990. Identification and characterization of the virion protein products of herpes simplex virus type 1 gene UL47. J. Gen. Virol. **71:**2953–2960.

11. **Mears, W. E., and S. A. Rice.** 1998. The herpes simplex virus immediate-early protein ICP27 shuttles between nucleus and cytoplasm. Virology **242:**128–137.

12. **Meyer, B. E., and M. H. Malim.** 1994. The HIV-1 Rev trans-activator shuttles between the nucleus and the cytoplasm. Genes Dev. **8:**1538–1547.

13. **Phelan, A., and J. B. Clements.** 1997. Herpes simplex virus type 1 immediate early protein IE63 shuttles between nuclear compartments and the cytoplasm. J Gen. Virol. **78:**3327–3331.

14. **Pinol-Roma, S., and G. Dreyfuss.** 1993. hnRNP proteins: localization and transport between the nucleus and the cytoplasm. Trends Cell Biol. **3:**151–155.

15. **Pinol-Roma, S., and G. Dreyfuss.** 1992. Shuttling of pre-mRNA binding proteins between nucleus and cytoplasm. Nature **355:**730–732.

16. **Pinol-Roma, S., and G. Dreyfuss.** 1991. Transcription-dependent and transcription-independent nuclear transport of hnRNP proteins. Science **253:**312–314.

17. **Rosin-Arbesfeld, R., A. Cliffe, T. Brabletz, and M. Bienz.** 2003. Nuclear export of the APC tumour suppressor controls beta-catenin function in transcription. EMBO J. **22:**1101–1113.

18. **Sandri-Goldin, R. M.** 1998. ICP27 mediates HSV RNA export by shuttling through a leucine-rich nuclear export signal and binding viral intronless RNAs through an RGG motif. Genes Dev. **12:**868–879.

19. **Sciortino, M. T., B. Taddeo, A. P. Poon, A. Mastino, and B. Roizman.** 2002. Of the three tegument proteins that package mRNA in herpes simplex virions, one (VP22) transports the mRNA to uninfected cells for expression prior to viral infection. Proc. Natl. Acad. Sci. USA **99:**8318–8323.

20. **Soliman, T. M., R. M. Sandri-Goldin, and S. J. Silverstein.** 1997. Shuttling of the herpes simplex virus type 1 regulatory protein ICP27 between the nucleus and cytoplasm mediates the expression of late proteins. J. Virol. **71:**9188–9197.

21. **van Drogen, F., and M. Peter.** 2001. MAP kinase dynamics in yeast. Biol. Cell. **93:**63–70.

22. **van Drunen Littel-van den Hurk, S., S. Garzon, J. V. van den Hurk, L. A. Babiuk, and P. Tijssen.** 1995. The role of the major tegument protein VP8 of bovine herpesvirus-1 in infection and immunity. Virology **206:**413–425.

23. **Whittaker, G. R., M. P. Riggio, I. W. Halliburton, R. A. Killington, G. P. Allen, and D. M. Meredith.** 1991. Antigenic and protein sequence homology between VP13/14, a herpes simplex virus type 1 tegument protein, and gp10, a glycoprotein of equine herpesvirus 1 and 4. J. Virol. **65:**2320–2326.

24. **Zhang, Y., and J. L. McKnight.** 1993. Herpes simplex virus type 1 UL46 and UL47 deletion mutants lack VP11 and VP12 or VP13 and VP14, respectively, and exhibit altered viral thymidine kinase expression. J. Virol. **67:**1482–1492.

25. **Zhang, Y., D. A. Sirko, and J. L. McKnight.** 1991. Role of herpes simplex virus type 1 UL46 and UL47 in alpha TIF-mediated transcriptional induction: characterization of three viral deletion mutants. J. Virol. **65:**829–841.

26. **Zheng, C., R. Brownlie, L. A. Babiuk, and S. van Drunen Littel-van den Hurk.** 2004. Characterization of nuclear localization and export signals of the major tegument protein VP8 of bovine herpesvirus-1. Virology **324:**327–339.